JACS
JOURNAL OF THE AMERICAN CHEMICAL SOCIETY
pubs.acs.org/JACS
Article

Discovery and Biosynthesis of Streptosactin, a Sactipeptide with an Alternative Topology Encoded by Commensal Bacteria in the Human Microbiome

Leah B. Bushin, Brett C. Covington, Britta E. Rued, Michael J. Federle, and Mohammad R. Seyedsayamdost*

Cite This: J. Am. Chem. Soc. 2020, 142, 16265−16275
Read Online

ABSTRACT: Mammalian microbiomes encode thousands of biosynthetic gene clusters (BGCs) and represent a new frontier in natural product research. We recently found an abundance of quorum sensing-regulated BGCs in mammalian microbiome streptococci that code for ribosomally synthesized and post-translationally modified peptides (RiPPs) and contain one or more radical S-adenosylmethionine (RaS) enzymes, a versatile superfamily known to catalyze some of the most unusual reactions in biology. In the current work, we target a widespread group of streptococcal RiPP BGCs and elucidate both the reaction carried out by its encoded RaS enzyme and identify its peptide natural product, which we name streptosactin. Streptosactin is the first sactipeptide identified from *Streptococcus* spp.; it contains two sequential four amino acid sactionine macrocycles, an unusual topology for this compound family. Bioactivity assays reveal potent but narrow-spectrum activity against the producing strain and its closest relatives that carry the same BGC, suggesting streptosactin may be a long-suspected fratricidal agent of *Streptococcus thermophilus*. Our results highlight mammalian streptococci as a rich source of unusual enzymatic chemistries and bioactive natural products.

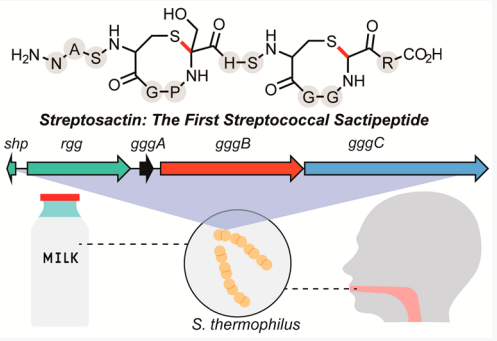

INTRODUCTION

Natural products remain a tremendous source of therapeutic agents and chemical tools with which to investigate biological phenomena.[1,2] For decades, discovery of natural products relied on screens of biological activity or chemical novelty. More recently, advances in DNA sequencing technologies and bioinformatics have reinvigorated the field by providing an alternative gene-first or genome-first approach. Aside from providing new discovery protocols, these advances have revealed the hidden biosynthetic potential of talented producers such as *Streptomyces* spp. They have also brought microbial genera to the fore that have not traditionally been viewed as abundant sources of bioactive compounds.[3−7] Among these, bacterial members of the human microbiome are an especially intriguing source because the natural products they synthesize can have a direct impact on human health.[8,9] The next challenge in tapping into the biosynthetic potential encoded in our microbiomes is connecting the computationally identified BGCs to their small molecule products and elucidating the functions of these molecules.

A family of natural products that appears particularly amenable to the genome-first approach is the ribosomally synthesized and post-translationally modified peptides (RiPPs).[10−12] RiPPs are generated by a biosynthetic framework that is conserved in all domains of life: A precursor peptide is synthesized by the ribosome from the canonical 20 amino acids. It is then modified by one or more tailoring enzymes, usually including a final proteolytic step to deliver the mature product.[13] A main advantage in mining for RiPPs when compared to other classes is that the substrate of the biosynthetic pathway, the precursor peptide, is genetically encoded and can therefore be easily predicted. Reactions catalyzed by the tailoring enzymes can then be characterized, thus providing valuable information in the hunt for the natural product.[14,15]

We previously conducted a bioinformatic search for RiPPs encoded by *Streptococcus* spp., an abundant genus in human and mammalian microbiomes and an underexamined source of natural products.[16] Our strategy was inspired by the BGC of streptide, a quorum sensing (QS) regulated macrocyclic peptide produced by the commensal bacterium *Streptococcus thermophilus* LMD-9.[17,18] Two features of the streptide BGC

Received: May 21, 2020
Published: August 26, 2020

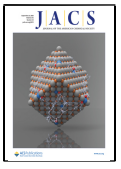

(*str*), the radical S-adenosylmethionine (RaS) enzyme and the *shp*/*rgg* QS operon, anchored our search. RaS enzymes harness a potent oxidant, the 5′-deoxyadenosyl radical (5′-dA•), to initiate a plethora of challenging reactions.[19−22] In streptide biosynthesis, for example, the RaS enzyme StrB introduces a carbon−carbon bond at unactivated positions between the side chains of lysine and tryptophan.[18,23,24] With only a fraction of its >500 000 members characterized, the RaS enzyme superfamily appeared ripe for the discovery of new and unusual chemistries.[25] *Shp*/*rgg* QS operons are specific to streptococci and regulate a variety of community behaviors, including competence, biofilm formation, and virulence.[26−32] We reasoned that natural products associated with QS-regulated, RaS enzyme-encoding clusters were likely to be chemically novel and physiologically relevant. Moreover, knowledge of their regulation would facilitate efforts to control production and thereby identify the mature product.

To find all *str*-like BGCs, 2785 streptococcal genomes in the Integrated Microbial Genomes and Microbiomes database were analyzed for colocalized instances of *shp*/*rgg* operons and genes coding for RaS enzymes.[16,33] Precursor peptides in the intergenic regions were then identified and mapped to give ∼600 such RiPP-encoding BGCs, which were organized in a sequence similarity network using the EFI-EST tool according to the precursor peptide sequences.[34,35] This 'RaS-RiPPs' network consists of 16 distinct subfamilies, suggesting 16 groups of RiPP natural products, which are named based on conserved motifs in the precursor peptides (Figure 1a). Our subsequent characterization of several subfamilies within the network has indeed uncovered an assortment of new modifications, including installation of an unprecedented tetrahydro[5,6]benzindole motif (*WGK*), a β-thioether linkage (*NxxC*), an α-ether cross-link (*TQQ*), and a carbon−carbon bond between the side chains of tyrosine and arginine (*RRR*) (Figure 1a).[16,36−38] While the reactions carried out by RaS enzymes within these subfamilies have been determined, the associated natural products have not yet been identified. Herein, we investigate the *GGG* subfamily and report both the reaction carried out by the RaS enzyme GggB as well as the structure of the mature natural product. Biosynthetic investigations reveal GggB to function as a sactisynthase that installs two consecutive α-thioether cross-links on its peptide substrate with a new topology for sactipeptides. Knowledge of the transformation enabled the discovery of the mature product, the first streptococcal sactipeptide, which we have named streptosactin. Elucidation of the timing of streptosactin synthesis and detection of antimicrobial activity against the producing host and closely related strains, which also harbor the *ggg* cluster, suggest this sactipeptide may be a fratricidal agent in *S. thermophilus*.

RESULTS AND DISCUSSION

***GGG* Subfamily.** As outlined above, the network in Figure 1a represents the landscape of RaS enzyme-synthesized and *shp*/*rgg*-controlled RiPPs. Of the 16 subfamilies, *GGG* is the fourth largest and comprises 35 gene clusters (Figure 1a). Most of these (∼20) are found in various *S. thermophilus* strains, nonpathogenic bacteria that are widely used starter cultures in dairy fermentation. They are also often identified as a natural constituent of milk, notably from cow and sheep.[39−41] The *ggg* cluster is also found in members of the human oral microbiome, including some strains of *Streptococcus constellatus*, *Streptococcus gordonii*, *Streptococcus oralis*, and *Streptococcus*

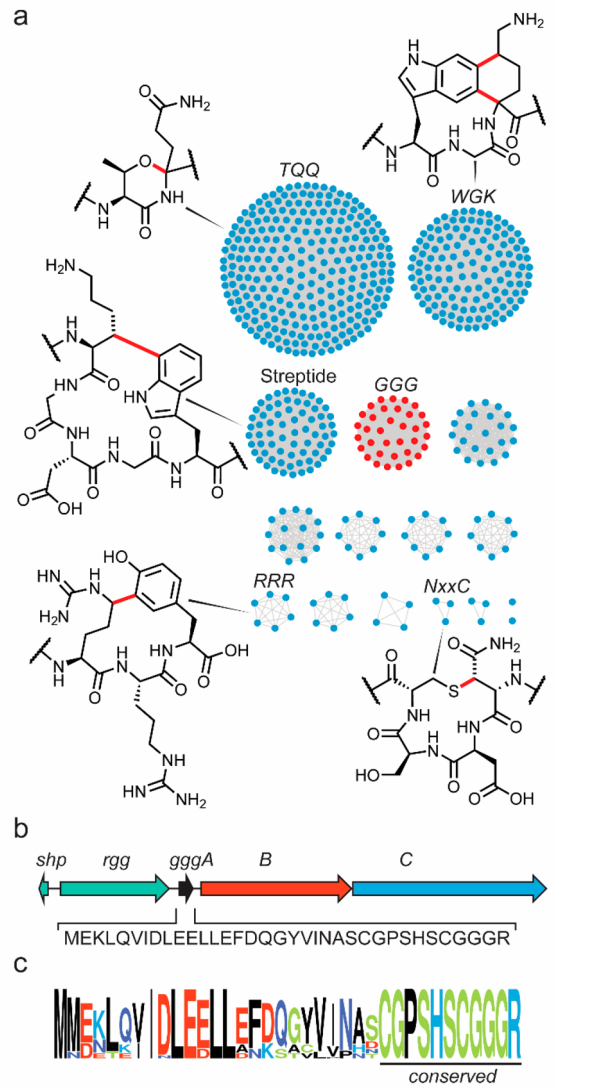

Figure 1. RaS enzyme-modified RiPPs in streptococci. (a) Sequence similarity network of RaS-RiPPs grouped according to precursor peptide sequences. With the exception of streptide, subfamilies are named on the basis of conserved motifs within the precursor peptide. The *GGG* subfamily is shown in red. (b) The *ggg* gene cluster from *S. thermophilus* JIM 8232. An *shp*/*rgg* operon (green) regulates production of the mature RiPP, encoded by a precursor peptide (black), a RaS enzyme (red), and a transporter (blue). (c) A sequence logo plot of the 35mer precursor peptide (GggA) shows that the 11 C-terminal residues are conserved.

parasanguinis. These bacteria are commensal in the oral cavity but can be pathogenic at other body sites.[42,43] The *ggg* locus in *S. thermophilus* encodes a 35mer precursor peptide (GggA), a RaS enzyme (GggB), and a transporter/protease (GggC) and is regulated by an upstream *shp*/*rgg* gene pair (Figure 1b). The 11 C-terminal residues of the precursor peptide are conserved within the subfamily, as depicted in the precursor peptide logo plot (Figure 1c). We focused on the *ggg* cluster from *S. thermophilus* JIM 8232, which was originally isolated from milk.[44]

Characterization of GggB and the GggB Reaction. We began by examining the reaction catalyzed by the RaS enzyme GggB. N-terminally hexaHis-tagged GggB was expressed recombinantly in *E. coli*, purified anaerobically, and reconstituted with Fe and sulfide, as previously reported (Tables

https://dx.doi.org/10.1021/jacs.0c05546
J. Am. Chem. Soc. 2020, 142, 16265−16275

S1−S3).[45] A UV−visible absorption spectrum of reconstituted GggB showed a shoulder at 325 nm and a broad feature at 410 nm, consistent with the presence of at least one $[4Fe\text{-}4S]^{2+}$ cluster (Figure 2a). Quantification of Fe and labile sulfide revealed 9.1 ± 1.3 Fe and 8.3 ± 1.2 S^{2-} per protomer. An EPR spectrum of reduced GggB gave a signal with apparent axial symmetry (Figure 2b). Spectral simulation and deconvolution showed that the observed signal was a composite of three signals. The major component (~75%) with g = [2.03, 1.91, 1.88] is indicative of a $[4Fe\text{-}4S]^{+}$ cluster routinely found in RaS enzymes and responsible for activation of S-adenosylmethionine (SAM, Figure 2b). Two minor components were also identified, one (~15%) with g = [2.04, 1.94, 1.89], consistent with another $[4Fe\text{-}4S]^{+}$, and a second (~10%) with g = [2.03, 2.01, 2.00], consistent with a $[3Fe\text{-}4S]^{+}$ cluster (Figure 2b) and likely the result of incomplete reconstitution or degradation of a [4Fe-4S] cluster. These data are in line with bioinformatic dissection of GggB, which predicts one active site $[4Fe\text{-}4S]^{+}$ cluster involved in the reductive cleavage of SAM and two Fe−S clusters in its C-terminal SPASM domain (Figure S1).[46−49] The exact nature of these SPASM domain clusters remains to be determined.

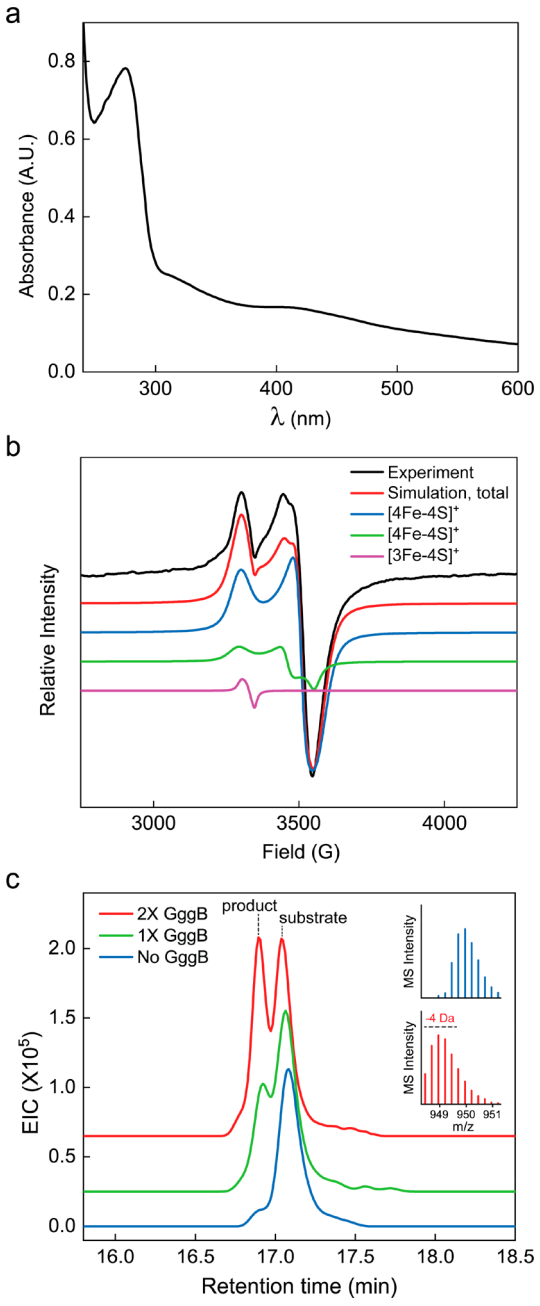

Figure 2. Characterization of GggB. (a) UV−vis absorption spectrum of reconstituted GggB. A 325 nm shoulder and a 410 nm broad feature indicate the presence of at least one $[4Fe\text{-}4S]^{2+}$ cluster. (b) X-band EPR spectrum of reconstituted, reduced GggB (black trace). Spectral simulation traces are color-coded as indicated. Note that signals for two different $[4Fe\text{-}4S]^{+}$ clusters can be simulated. See text for g-values of the simulated spectra. (c) GggB enzymatic activity monitored by HPLC-Qtof-MS. Extracted ion chromatographs (EIC) of the $[M+3H]^{3+}$ ion for the substrate (m/z 1265.6010) and the −4 Da product (m/z 1264.2555) are shown. Formation of this product peak is GggB-dependent. Inset, HR-MS data focusing on the $[M+4H]^{4+}$ ion for the substrate (top, blue) and product (bottom, red).

With reconstituted GggB in hand, its reaction with the precursor peptide GggA was examined next. GggA was prepared by solid-phase peptide synthesis (SPPS), purified, and subsequently incubated with GggB, SAM, and reductant ($Na_2S_2O_4$) under anaerobic conditions. Analysis of the reaction components by HPLC-Qtof-MS revealed formation of a putative product that was 4 Da lighter than the substrate (Figure 2c, Table S4). This species was not present in the absence of GggB, consistent with its assignment as the reaction product.

Structural Elucidation of the GggB Product. Initial clues toward the structure of the reaction product were provided by tandem high-resolution mass spectrometry (HR-MS/MS). Collision-induced dissociation yielded y-ions for nearly the entire sequence of GggA but only b-ions for the N-terminal leader region (Figure 3a). All y-ions spanning His29 and Gly34 (Figure 3a, blue) lacked two hydrogens whereas those from the N-terminus to Ser28 lacked four, implicating Ser28 and Gly34 (Figure 3a, blue) as sites of modification (Table S5). Given the presence of a conserved Cys three amino acids upstream of each modified site (Figure 3a, red), we considered that these residues may be participating in thioether bonds. Indeed, the HR-MS/MS fragmentation pattern of the product was indicative of α-thioether bonds, also known as sactionine linkages, which undergo facile in-source retro-elimination during MS analysis, thus affording dehydrogenated acceptor residues and fragment ions within the macrocycle.[50−52]

To test whether the modifications consisted of α-thioether linkages, uniformly ^{13}C-labeled amino acids were incorporated into GggA by SPPS at the implicated positions, Ser28 and Gly34. Each site-specifically labeled variant was reacted with GggB and subjected to HR-MS/MS and NMR analysis. HR-MS/MS was consistent with two macrocycles, also observed with unlabeled GggA (Table S6). A 1D ^{13}C-spectrum of $^{15}N,^{13}C_2$-Gly34-GggA reacted with GggB showed two new peaks, which we attribute to the product (Figure 3b). The new Cα signal was shifted downfield relative to substrate from 42.5 to 54.0 ppm. A DEPT-edited HSQC spectrum showed it was a methine-carbon and gave the chemical shift of the associated Hα at 5.48 ppm (Figures S2, S3, Table S7). The shift of the new carbonyl was only slightly upfield (167.8 ppm) relative to substrate but within range for a typical peptide bond. These results along with other chemical shifts (Table S7) were fully consistent with formation of sactionine bridge at Gly34.

https://dx.doi.org/10.1021/jacs.0c05546
J. Am. Chem. Soc. 2020, 142, 16265−16275

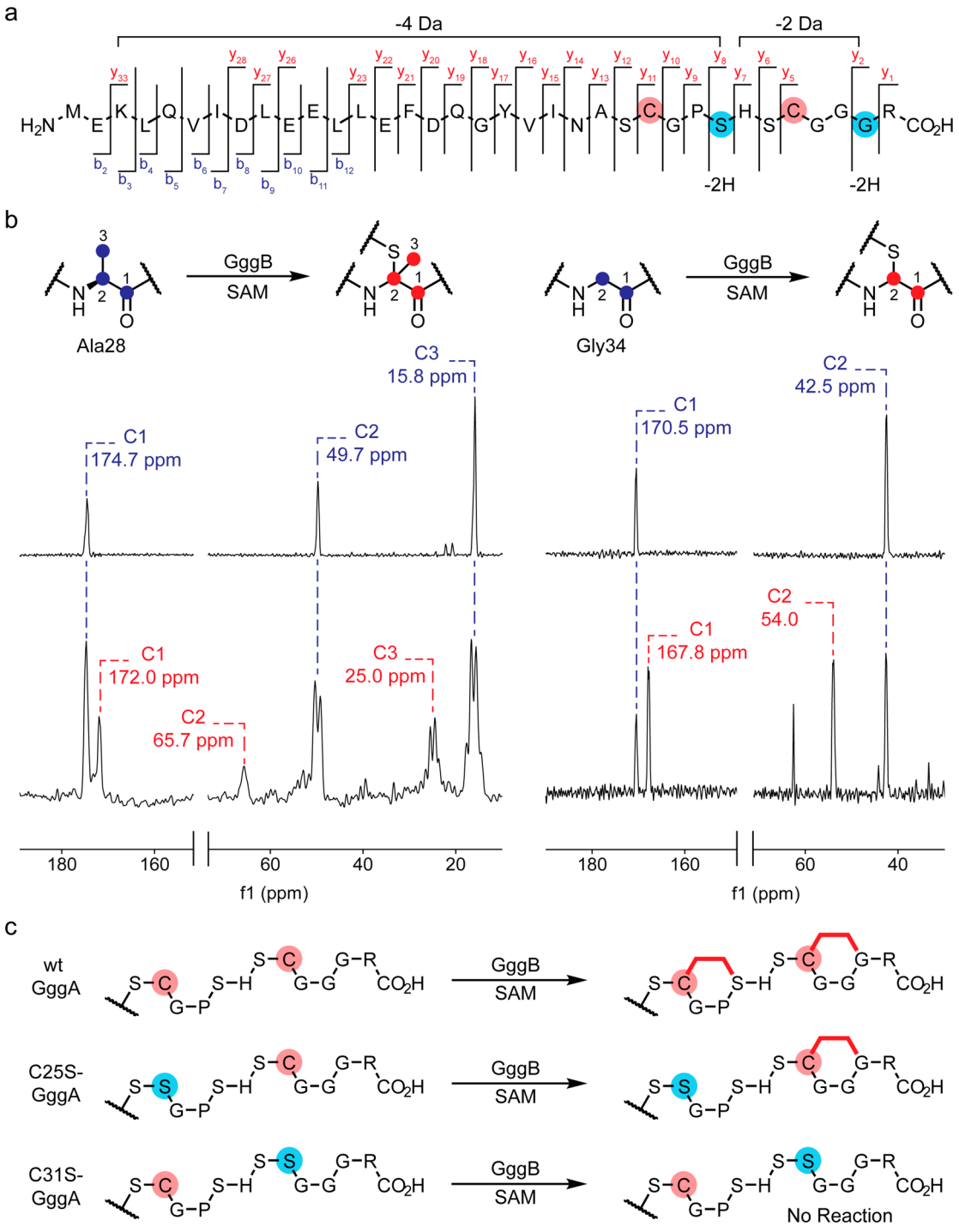

Figure 3. Structural elucidation of the GggB product. (a) HR-MS/MS analysis of the GggB product shows that fragments y2-y7 and y8-y33 are 2 Da and 4 Da, respectively, lighter than the same fragments derived from the substrate. The pattern points to modifications at residues Ser28 and Gly34 (highlighted with blue spheres). (b) Stacked ^{13}C NMR spectra of $^{13}C_3$-A28-GggA (left) and $^{13}C_2$-G34-GggA (right) before (top) and after (bottom) reaction with GggB. Peaks are assigned to substrate (blue) or product (red), with the carbon position and chemical shift values labeled. The numbering schemes for the isotopically labeled residues are shown. (c) Reaction of GggB with wt GggA (top), C25S-GggA (middle), and C31S-GggA (bottom). The Ser25 substitution prevents cross-linking at Ser28 whereas the Ser31 substitution precludes formation of both cross-links.

Due to the lack of availability of Ser isotopologues, we explored a Ser28Ala substitution at the second site of modification. Reaction of S28A-GggA with GggB and analysis by HR-MS and HR-MS/MS revealed formation of a −4 Da product with a fragmentation pattern matching wild-type (wt) GggA, save for expected m/z shifts due to the Ala substitution at residue 28. This indicated that the Ser28Ala variant underwent the same cross-linking reaction (Tables S4, S8). Next, $^{13}C_3$−Ala was inserted by SPPS at residue 28 of GggA and reacted with GggB, and the reaction product was analyzed by NMR. We assigned a new peak at 65.7 ppm to the thioetherified Cα at Ala28, a shift from 49.7 ppm in the

https://dx.doi.org/10.1021/jacs.0c05546
J. Am. Chem. Soc. 2020, 142, 16265−16275

substrate (Figure 3b). Similarly Cβ of Ala28 was shifted from 15.8 to 25.0 ppm after reaction with GggB. These properties and correlations from a DEPT-edited HSQC spectrum (Figures S4, S5, Table S9) were entirely consistent with an S−Cα bond at Ala28.

Having confirmed the presence of the two sactionine linkages, we next used Cys-to-Ser substitutions in GggA to unequivocally determine the exact donor/acceptor pairings. This substitution is known to preclude crossbridge formation as sactisynthases do not install ether bonds in lieu of thioethers.[53,54] The sequence of GggA differs from those of known sactipeptides in that the cysteines and acceptor residues alternate along the peptide chain. Incubation of GggB with C25S-GggA generated a product that was only 2 Da lighter than the substrate with a single cross-link between Cys31 and Gly34, as determined by HR-MS/MS (Figure 3c, Tables S4, S10). To our surprise, no product was observed with C31S-GggA, suggesting that the installation of sactionine linkages occurs in a defined order from C- to N-terminus and that the formation of the second is dependent on the presence of the first. Together, these data demonstrate that GggB introduces a duo of α-thioether bonds between Cys31-Gly34 and Cys25-Ser28, building two adjacent 4-residue macrocycles in the core region of GggA. The absolute configuration at the thioetherified Cα of Gly34 and Ser28 remains to be defined.

Mechanistic Investigations. SkfB and AlbA are two well-studied sactisynthases involved in the production of the sporulation killing factor (SKF) and subtilosin, respectively.[53,54] Deuterium labeling studies by Bruender et al. recently demonstrated that SkfB initiates α-thioether bond formation via H-atom abstraction from the Cα of the acceptor residue (Figure S6).[55] To investigate if GggB installs α-thioether cross-links in a similar manner, we synthesized α-$^2H_2$-Gly34-GggA and examined its reaction with GggB. We observed formation of 5′-^{2}H-5′-deoxyadenosine (5′-^{2}H-5′-dA) and a product that was 5 Da lighter than substrate, consistent with deuterium transfer from the Cα of Gly34 to 5′-dA• (Figures 4a, S7, Tables S4, S11). Similar results were observed

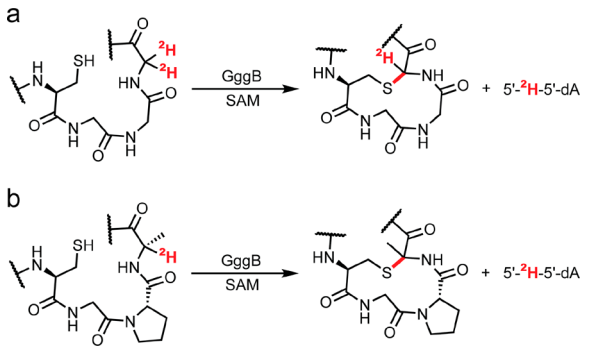

Figure 4. GggB-catalyzed H-atom abstraction from the Cα of acceptor residues by 5′-dA•. Reaction of GggB with 2-$^2H_2$-G34-GggA (a) or 2-^{2}H-A28-GggA (b) yields a product that is 5 Da lighter than substrate, and to formation of 5′-^{2}H-5′-dA.

with GggA carrying α-^{2}H-Ala at position 28 (Figures 4b, S7, Tables S4, S12). By contrast, when β-$^2H_3$−Ala was inserted at position 28, all three deuterons were retained in the product (Tables S4, S13), and only 5′-dA was observed, again consistent with abstraction of Hα but not Hβ. Given that 5′-^{2}H-5′-dA was detected upon labeling either Cα at Gly34 or Ala28, it appears that each cyclization reaction is initiated *de novo*, consuming one equivalent of SAM.

Following the generation of the substrate Cα radical, at least three distinct routes to sulfur insertion are plausible. In one pathway (mechanism A, Figure S6a), the Cys-SH, activated by ligation to an auxiliary Fe−S cluster, directly couples to the Cα• concomitant with the reduction of the auxiliary cluster. This mechanism was previously favored by Marahiel and co-workers.[53,54] Alternatively, oxidation of the substrate radical and deprotonation of the amide N−H bond could generate an electrophilic ketoimine intermediate, which is primed for nucleophilic attack by Cys-SH (mechanism B, Figure S6b). Finally, a ketoiminium can be generated without deprotonation of the radical-adjacent N−H (mechanism C, Figure S6c).[56] To investigate the involvement of the amide N−H bond, we tested the activity of GggB on *N*-methylated substrate analogs and found that methylation inhibited cross-link formation. Reactions with either N-Me-Ala28 or N-Me-Ser28 generated monocyclized products with cross-links at only Gly34, as determined by HR-MS and HR-MS/MS (Tables S4, S14). Reactions with N-Me-Gly34 generated no product at all.

Two conclusions may be drawn from these results. First, they confirm the order of cross-link formation described above, with GggB installing the modification at Gly34 and then at Ser28. And second, they hint at a role for the amide N−H in the catalytic cycle. Because the lack of product formation may be explained by steric perturbations, this experiment alone is not sufficient to differentiate between the mechanistic possibilities. Nonetheless, the requirement for a Cα radical and the importance of the N−H provide a framework for examining the mechanism of GggB and differentiating between pathways A−C in the future.

Engineered Processive Cyclizations by GggB. The modified region of GggA consists of two 6-residue stretches that are very similar in sequence (Figure 5a). The first 3 residues, (−SCG−) are conserved, followed by a helix breaker (P/G), an acceptor (S/G), and a basic residue (H/R). We imagined that this "consensus sequence" could be exploited to manipulate the number of cyclizations catalyzed by GggB. As the preparation of longer peptides by SPPS would be onerous, we opted to carry out the reactions heterologously by coexpressing GggB and the respective GggA variant from the same plasmid in *E. coli*. The reaction would take place in the context of the cytosol and the product would then be purified using affinity chromatography.[57] We previously used this type of construct to investigate the *rrr* gene cluster from *Streptococcus suis*.[38]

GggA was furnished with a hexaHis-maltose binding protein (6HMBP) tag to enhance solubility and facilitate purification of the reaction product from cell lysates. GggB was encoded on the same plasmid, the expression of both genes being controlled by a *lac* promoter (Figure 5b). After confirming the efficiency of the system with wt GggA (Tables S15−S17), we tested GggA variants with an increasing number of 6-residue consensus sequence units from 1 to 4 (Figure 5c). For simplicity, we used only the sequence "SCGGGR". Interestingly, GggB installed a cross-link on every iteration of the consensus sequence, from 1 cross-link on the shortest variant to 4 cross-links on the longest variant (Figure 5c, Tables S15−S21). When the stretch of 6mer sequences was interrupted with a sequence that did not contain a Cys residue, cross-link formation stalled. In the final construct listed, for example (Figure 5d, Table S22), only a single sactionine was installed at

https://dx.doi.org/10.1021/jacs.0c05546
J. Am. Chem. Soc. 2020, 142, 16265−16275

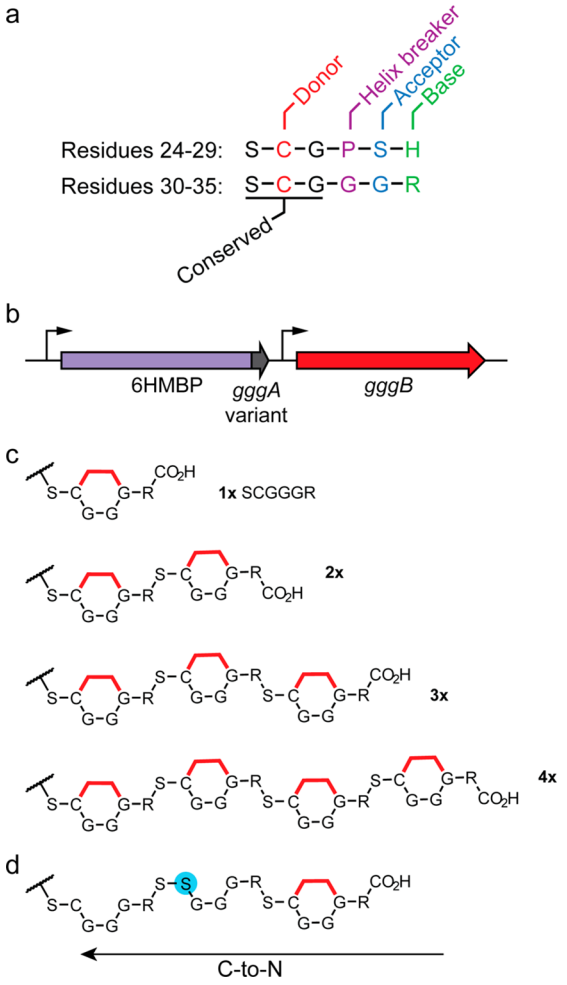

Figure 5. Processivity of GggB. (a) Alignment of residues 24−29 and residues 30−35 reveals a consensus sequence on which GggB acts to install a thioether cross-link. (b) Expression region of the plasmid used to carry out the GggAB reaction heterologously. One *lac* operon codes for GggA that is N-terminally fused to a 6HMBP tag; the other codes for GggB. (c) Reaction outcomes for 6HMBP-GggA fusions containing 1, 2, 3, or 4 "SCGGGR" units. GggB installs a thioether bond at every instance of the unit, generating products with 1, 2, 3, and 4 macrocycles. (d) A Cys-to-Ser substitution in the second unit of the 3-unit variant gives a monocyclic product and stalls GggB.

the C-terminus. These results suggest that GggB recognizes the consensus sequence and installs the thioether bond from C- to N-terminus in a processive manner regardless of the length of the precursor. It will be of interest to examine the role of the leader peptide and the RiPP recognition element in this process in the future.

Discovery of Streptosactin, the Mature *ggg* Product. The results thus far demonstrate the reaction carried out by GggB and provide clues toward its catalytic mechanism. With knowledge of the structure of the GggB product, we next set out to identify the mature peptide secreted by *S. thermophilus* JIM 8232. Cultures of this bacterium were grown to late exponential phase (see below) and targeted HR-MS analysis was conducted on the resulting cell-free supernatants. Specifically, based on the logic of RiPP biogenesis, we hypothesized that GggC would cleave doubly cross-linked GggA at a residue N-terminal to Cys25, but not further upstream than Phe15, beyond which there is a cluster of acidic residues. We computationally assembled a list of nine *m*/*z* values for the possible mature product and searched for these in the *S. thermophilus* supernatants. The molecular ions thus identified were subjected to HR-MS/MS analysis. Only one candidate emerged from these experiments, corresponding to the doubly cross-linked C-terminal 14mer (Figure 6a, top trace); it displayed HR-MS and fragmentation patterns highly analogous to that of the enzymatic product (Table S23). The abundance of the natural product, however, was prohibitively low for confirmation of the structure by NMR spectroscopy. We therefore opted to prepare the putative mature product and assess its chromatographic and HR-MS properties in comparison to the authentic material.

Synthesis of the doubly cross-linked 14mer took advantage of our heterologous coexpression system described above (Figure 5b). To generate a 14mer, an Arg residue was inserted into the GggA sequence just before Asn22 such that proteolysis with trypsin, which hydrolyzes peptide bonds at the carboxyl group of basic residues, would afford the desired peptide. Coexpression of this modified peptide with GggB, subsequent trypsinolysis, and purification by HPLC provided the doubly cross-linked 14mer in approximately 1 mg yield from a 15 L *E. coli* culture (Table S24). 1*D*/2D NMR analysis of this 14mer peptide showed features identical to the GggB product characterized above, confirming it was the doubly cyclized peptide containing the same sactionine linkages (Figure S8). This standard was then compared with the authentic material from *S. thermophilus* JIM 8232; it showed identical chromatographic behavior and coeluted with the authentic natural product, when injected in a 1:1 ratio (Figure 6a). It also exhibited similar HR-MS and HR-MS/MS properties (Tables S23, S25), supporting the same amino acid sequence and structure. Together, these studies establish the structure of the mature natural product from the *ggg* cluster (Figure 6b,c). This 14mer RiPP, which we have named streptosactin, is the first sactipeptide of streptococcal origin. It forms a new subclass of sactipeptides: as recently pointed out by Hudson et al.,[12] all sactipeptides discovered thus far consist of a hairpin topology in which thioether cross-links are nested such that the most upstream (N-terminal) Cys residue reacts with the most downstream (C-terminal) acceptor. In streptosactin, however, the Cys donors and acceptors alternate along the core peptide, yielding a distinct "bicycle" topology of unnested macrocycles (Figure 6d). We propose classification of sactipeptides with the hairpin topology as type 1 and those with the new streptosactin-like topology as type 2.

Streptosactin: Timing of Production and Antimicrobial Activity. Like all BGCs in the network in Figure 1, the *ggg* locus is controlled by an *shp*/*rgg* QS operon, which suggests that streptosactin synthesis is positively regulated by cell density. We tested this prediction by quantifying streptosactin production as a function of *S. thermophilus* growth phase, as determined by optical density at 600 nm (OD_{600}). Indeed, streptosactin levels in the supernatant increased with cell density as a rapid rise was observed between 12 and 15 h, with streptosactin concentrations peaking at late exponential phase, beyond which point they decreased slowly over several days (Figure 7a). The role of *rgg*, and therefore QS, in this process remains to be determined. The low levels of the sactipeptide, which we determined using a standard curve with synthetic material, provide an explanation as to why purification and structural elucidation of authentic streptosactin was not possible. We do note that the concentration shown (Figure 7a) represents a lower limit,

https://dx.doi.org/10.1021/jacs.0c05546
J. Am. Chem. Soc. 2020, 142, 16265−16275

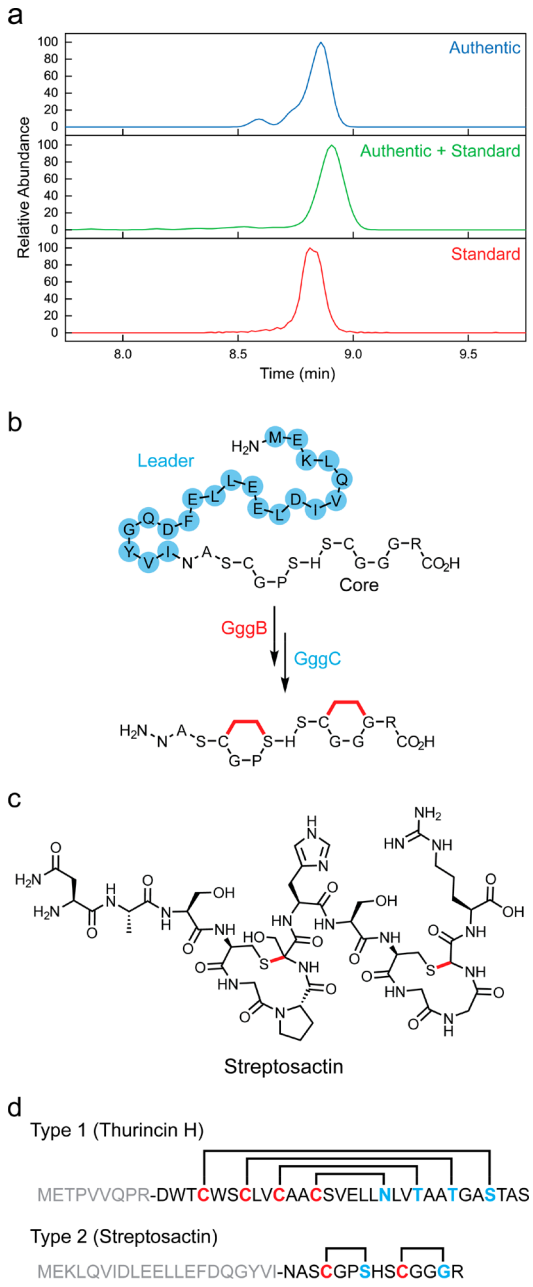

Figure 6. Identification of streptosactin, the mature product of the *ggg* cluster. (a) HPLC-Qtof-MS analysis of authentic and synthetic streptosactin. Shown are extracted ion chromatograms for authentic streptosactin from *S. thermophilus* JIM 8232 (blue, top), heterologously produced streptosactin (red, bottom), and a 1:1 coinjection of these two samples (green, middle), which coelute. (b) Proposed biosynthesis of streptosactin. GggB installs two thioether bonds in the core region of GggA. A protease, likely GggC, removes the leader (blue spheres), affording the mature 14mer product. (c) Structure of streptosactin. Absolute configurations at the α-carbons of the acceptor residues remain to be determined. (d) Comparison of the topology of known "type 1" sactipeptides, with thurincin H as a representative example, and the new type 2 streptosactin. Leader sequences are shown in gray.

as some material is likely lost during workup and detection. Moreover, this bulk concentration in a laboratory monoculture is not necessarily indicative of the levels of streptosactin under physiological conditions.

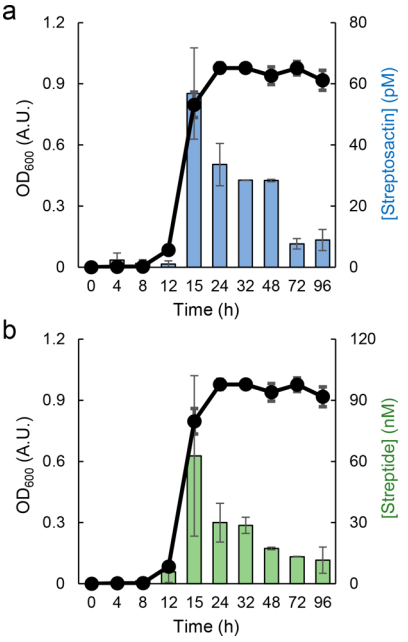

Figure 7. QS-regulated production of streptosactin and streptide by *S. thermophilus* JIM 8232. Biosynthesis of streptosactin (a, blue bars) or streptide (b, green bars) as a function of OD_{600} (black traces). The averages of three independent measurements are shown; bars represent standard error.

S. thermophilus JIM 8232 also encodes *str*, though streptide production has not yet been shown in this strain. The *str* BGC is also downstream of an *shp/rgg* operon. We therefore monitored the supernatants of this strain, identified streptide, and observed production patterns very similar to those of streptosactin, with a rapid early increase, optimal streptide concentrations in late exponential phase, followed by a steady decline during stationary phase (Figure 7b). The *shp/rgg* circuits in *S. thermophilus*, therefore, appear to optimize streptide and streptosactin synthesis in late exponential phase. It is unclear whether the decline in streptide and streptosactin in stationary phase is due to spontaneous degradation, reuptake, or enzyme-mediated decomposition.

S. thermophilus primarily resides in oral and nasal passages. In exploring the bioactivity of streptosactin, we focused on its effects on the growth behavior of 15 other firmicutes (Table S26) that share these body sites and compete with *S. thermophilus*.[58] Because our studies suggested limited endogenous production of streptosactin, we tested low titers (0.1 μM and 1 μM) against other bacteria. We observed no significant effects on the growth kinetics of most strains tested (Figure 8). Growth of *Streptococcus sanguinis* was affected by streptosactin, although the control grew poorly in our hands. Clearly, most affected by streptosactin, however, was the growth of *S. thermophilus* LMD-9 and *S. thermophilus* LMG 18311, with 1 μM causing complete growth inhibition (Figure 8g). Interestingly, these strains both encode a *ggg* cluster with GggA precursor peptide sequences that are identical to that of *S. thermophilus* JIM 8232. When tested against strain JIM 8232, streptosactin showed similar growth-inhibitory activity (Figure 8h), an unusual case of a toxin killing the producing host when provided during prelogarithmic growth. In addition to growth inhibition, cell clumps were observed in a streptosactin-dependent manner (Figure S9).

https://dx.doi.org/10.1021/jacs.0c05546
J. Am. Chem. Soc. 2020, 142, 16265−16275

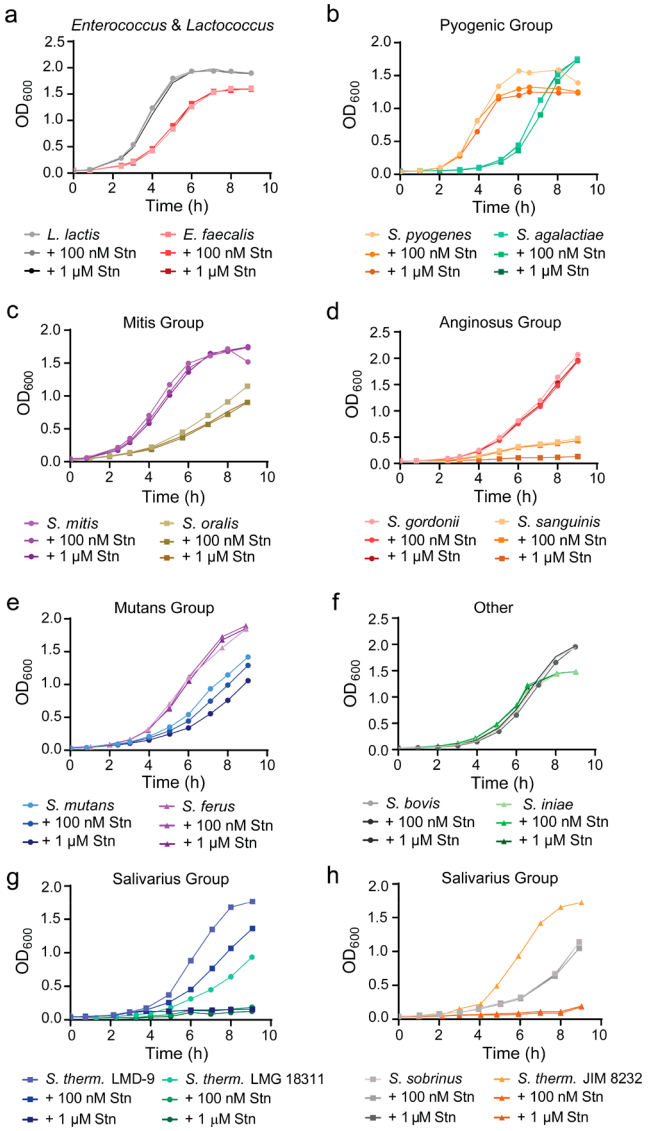

Figure 8. Effect of streptosactin on the growth kinetics of 15 firmicutes. Shown are effects of media-control, 0.1 μM, or 1 μM streptosactin on *E. faecalis* and *L. lactis* (a), *S. pyogenes* and *S. agalactiae* (b), *S. mitis* and *S. oralis* (c), *S. gordonii* and *S. sanguinis* (d), *S. mutans* and *S. ferus* (e), *S. bovis* and *S. iniae* (f), *S. thermophilus* LMD-9 and *S. thermophilus* LMG 18311 (g), and *S. sobrinus* and *S. thermophilus* JIM 8232 (h).

The unusual property of streptosactin of killing the producer cells provides an important clue in interpreting the function of this sactipeptide. The timing of streptosactin and streptide synthesis correlates well with the development of competence, which has been reported from *S. thermophilus* by several groups.[59−62] Indeed, in a previous study, expression of the *ggg* locus was found to correlate with those of early competence genes in *S. thermophilus* LMD-9.[59] Competence, the ability to pick up environmental DNA and incorporate it into the chromosome, is controlled by the *comRS* operon, also an *shp/rgg* system in *S. thermophilus*.[59] Competence is associated with fratricide; that is, killing of noncompetent sister cells by competent ones, a process that releases DNA into the environment, which can be taken up and incorporated.[63−67] The agents of fratricide, known as fratricins, have been well-characterized in *Streptococcus pneumoniae*, where they have been shown to consist primarily of hydrolytic enzymes (type III bacteriocins) and to a lesser extent medium-length unmodified peptides (type II bacteriocins).[63−67] *S. thermophilus* does not encode the typical set of fratricins and it has been proposed to encode alternative ones.[67,68] The correlated production of streptosactin with the development of the competent state, the potent self-killing activity of this sactipeptide, and even the cell clumping phenotype, which occurs when DNA is released into the medium,[65,69] all lead us to propose streptosactin as the first fratricidal agent in *S. thermophilus*.

CONCLUSION

Our bioinformatic search for QS-regulated and RaS enzyme-modified RiPPs identified streptococci as an abundant source. This finding was rather surprising as the capacity for natural product biosynthesis is typically correlated with genome size.[7] With small, host-adapted genomes around 1.8 Mbp, streptococci were not thought of as prolific producers. RiPP BGCs, however, are the ideal small molecule tools for streptococci as they have modest genomic footprints and allow for synthesis of complex natural products. The identification of streptide and streptosactin from *S. thermophilus*, the use of short hydrophobic peptides to control the synthesis of these molecules, and the presence of two additional RaS-RiPP BGCs in this strain are in line with the notion of streptococci using RiPPs as a language to communicate and compete with other streptococci.

Streptosactin joins the growing list of sactipeptides first structurally elucidated by Vederas and co-workers.[70,71] Seven sactipeptide natural products have been characterized to date: subtilosin, SKF, thuricin α and β, thurincin H, huazacin/thuricin Z, and ruminococcin C, all produced by *Bacillus* species with the exception of the latter, which is synthesized by *Ruminococcus gnavus*.[12,50,72−77] The sactipeptide natural products thus far exhibit a nested hairpin topology. As the first streptococcal sactipeptide to comprise an unnested bicycle topology, streptosactin bucks both trends. In the current work, we explored the biosynthesis and biological activity of streptosactin. We show that GggB installs the sactionine linkages in an ordered fashion and report narrow-spectrum, fratricidal activity for the mature product. Although the *ggg* BGC is not regulated by competence, the upstream *shp/rgg* locus could provide a synchronization device, as previously proposed, to correlate streptosactin synthesis with expression of competence genes.[59,62] Other functions for streptosactin cannot be ruled out, especially in the complex environment of mammalian microbiomes, and these remain to be investigated. Aside from addressing the absolute configuration of streptosactin's sactionine linkages and enhancing our understanding of its function, future studies will continue to mine the streptococcal RaS-RiPPs network (Figure 1) as a rich source of novel enzymatic chemistries and natural products as well as their associated ecological roles.

ASSOCIATED CONTENT

Supporting Information

The Supporting Information is available free of charge at https://pubs.acs.org/doi/10.1021/jacs.0c05546.

Complete Material and Methods, including procedures used for expression and purification of GggB, solid-phase peptide synthesis of GggA and isotopologues, enzymatic

https://dx.doi.org/10.1021/jacs.0c05546
J. Am. Chem. Soc. 2020, 142, 16265−16275

activity assays, mechanistic studies, structural elucidation of the GggB product, heterologous expression of GggAB, identification of streptosactin and streptide from *S. thermophilus* JIM 8232, quantification of streptide and streptosactin in bulk solution, biological activity assays with streptosactin (PDF)

AUTHOR INFORMATION

Corresponding Author

Mohammad R. Seyedsayamdost − *Department of Chemistry and Department of Molecular Biology, Princeton University, Princeton, New Jersey 08544, United States;* orcid.org/0000-0003-2707-4854; Email: mrseyed@princeton.edu

Authors

Leah B. Bushin − *Department of Chemistry, Princeton University, Princeton, New Jersey 08544, United States*

Brett C. Covington − *Department of Chemistry, Princeton University, Princeton, New Jersey 08544, United States*

Britta E. Rued − *Department of Pharmaceutical Sciences, University of Illinois at Chicago, Chicago, Illinois 60607, United States*

Michael J. Federle − *Department of Pharmaceutical Sciences, University of Illinois at Chicago, Chicago, Illinois 60607, United States*

Complete contact information is available at: https://pubs.acs.org/10.1021/jacs.0c05546

Notes

The authors declare no competing financial interest.

ACKNOWLEDGMENTS

The authors are grateful to Ryan J. Martinie for assistance with EPR spectral simulation, the National Science Foundation (NSF GRFP Award to L.B.B. and NSF CAREER Award to M.R.S.), and the Burroughs Wellcome Fund PATH Investigator Award (to M.J.F. and M.R.S.) for support of this work.

REFERENCES

(1) Newman, D. J.; Cragg, G. M. Natural Products as Sources of New Drugs over the Nearly Four Decades from 01/1981 to 09/2019. *J. Nat. Prod.* **2020**, *83*, 770−803.

(2) Carlson, E. E. Natural Products as Chemical Probes. *ACS Chem. Biol.* **2010**, *5*, 639−653.

(3) Clardy, J.; Walsh, C. Lessons from Natural Molecules. *Nature* **2004**, *432*, 829−837.

(4) Doroghazi, J. R.; Albright, J. C.; Goering, A. W.; Ju, K.-S.; Haines, R. R.; Tchalukov, K. A.; Labeda, D. P.; Kelleher, N. L.; Metcalf, W. W. A Roadmap for Natural Product Discovery Based on Large-Scale Genomics and Metabolomics. *Nat. Chem. Biol.* **2014**, *10*, 963−968.

(5) Harvey, A. L.; Edrada-Ebel, R.; Quinn, R. J. The Re-Emergence of Natural Products for Drug Discovery in the Genomics Era. *Nat. Rev. Drug Discovery* **2015**, *14*, 111−129.

(6) Katz, L.; Baltz, R. H. Natural Product Discovery: Past, Present, and Future. *J. Ind. Microbiol. Biotechnol.* **2016**, *43*, 155−176.

(7) Baltz, R. H. Gifted Microbes for Genome Mining and Natural Product Discovery. *J. Ind. Microbiol. Biotechnol.* **2017**, *44*, 573−588.

(8) Donia, M. S.; Cimermancic, P.; Schulze, C. J.; Wieland Brown, L. C.; Martin, J.; Mitreva, M.; Clardy, J.; Linington, R. G.; Fischbach, M. A. A Systematic Analysis of Biosynthetic Gene Clusters in the Human Microbiome Reveals a Common Family of Antibiotics. *Cell* **2014**, *158*, 1402−1414.

(9) Donia, M. S.; Fischbach, M. A. Small Molecules from the Human Microbiota. *Science* **2015**, *349*, 1254766.

(10) Maksimov, M. O.; Pelczer, I.; Link, A. J. Precursor-Centric Genome-Mining Approach for Lasso Peptide Discovery. *Proc. Natl. Acad. Sci. U. S. A.* **2012**, *109*, 15223−15228.

(11) Tietz, J. I.; Schwalen, C. J.; Patel, P. S.; Maxson, T.; Blair, P. M.; Tai, H.-C.; Zakai, U. I.; Mitchell, D. A. A New Genome-Mining Tool Redefines the Lasso Peptide Biosynthetic Landscape. *Nat. Chem. Biol.* **2017**, *13*, 470−478.

(12) Hudson, G. A.; Burkhart, B. J.; DiCaprio, A. J.; Schwalen, C. J.; Kille, B.; Pogorelov, T. V.; Mitchell, D. A. Bioinformatic Mapping of Radical S-Adenosylmethionine-Dependent Ribosomally Synthesized and Post-Translationally Modified Peptides Identifies New Cα, Cβ, and Cγ-Linked Thioether-Containing Peptides. *J. Am. Chem. Soc.* **2019**, *141*, 8228−8238.

(13) Arnison, P. G.; Bibb, M. J.; Bierbaum, G.; Bowers, A. A.; Bugni, T. S.; Bulaj, G.; Camarero, J. A.; Campopiano, D. J.; Challis, G. L.; Clardy, J.; Cotter, P. D.; Craik, D. J.; Dawson, M.; Dittmann, E.; Donadio, S.; Dorrestein, P. C.; Entian, K.-D.; Fischbach, M. A.; Garavelli, J. S.; Goransson, U.; Gruber, C. W.; Haft, D. H.; Hemscheidt, T. K.; Hertweck, C.; Hill, C.; Horswill, A. R.; Jaspars, M.; Kelly, W. L.; Klinman, J. P.; Kuipers, O. P.; Link, A. J.; Liu, W.; Marahiel, M. A.; Mitchell, D. A.; Moll, G. N.; Moore, B. S.; Muller, R.; Nair, S. K.; Nes, I. F.; Norris, G. E.; Olivera, B. M.; Onaka, H.; Patchett, M. L.; Piel, J.; Reaney, M. J. T.; Rebuffat, S.; Ross, R. P.; Sahl, H.-G.; Schmidt, E. W.; Selsted, M. E.; Severinov, K.; Shen, B.; Sivonen, K.; Smith, L.; Stein, T.; Sussmuth, R. D.; Tagg, J. R.; Tang, G.-L.; Truman, A. W.; Vederas, J. C.; Walsh, C. T.; Walton, J. D.; Wenzel, S. C.; Willey, J. M.; van der Donk, W. A. Ribosomally Synthesized and Post-Translationally Modified Peptide Natural Products: Overview and Recommendations for a Universal Nomenclature. *Nat. Prod. Rep.* **2013**, *30*, 108−160.

(14) Ortega, M. A.; van der Donk, W. A. New Insights into the Biosynthetic Logic of Ribosomally Synthesized and Post-Translationally Modified Peptide Natural Products. *Cell Chem. Biol.* **2016**, *23*, 31−44.

(15) Hetrick, K. J.; van der Donk, W. A. Ribosomally Synthesized and Post-Translationally Modified Peptide Natural Product Discovery in the Genomic Era. *Curr. Opin. Chem. Biol.* **2017**, *38*, 36−44.

(16) Bushin, L. B.; Clark, K. A.; Pelczer, I.; Seyedsayamdost, M. R. Charting an Unexplored Streptococcal Biosynthetic Landscape Reveals a Unique Peptide Cyclization Motif. *J. Am. Chem. Soc.* **2018**, *140*, 17674−17684.

(17) Ibrahim, M.; Guillot, A.; Wessner, F.; Algaron, F.; Besset, C.; Courtin, P.; Gardan, R.; Monnet, V. Control of the Transcription of a Short Gene Encoding a Cyclic Peptide in *Streptococcus thermophilus*: A New Quorum-Sensing System? *J. Bacteriol.* **2007**, *189*, 8844−8854.

(18) Schramma, K. R.; Bushin, L. B.; Seyedsayamdost, M. R. Structure and Biosynthesis of a Macrocyclic Peptide Containing an Unprecedented Lysine-to-Tryptophan Crosslink. *Nat. Chem.* **2015**, *7*, 431−437.

(19) Sofia, H. J.; Chen, G.; Hetzler, B. G.; Reyes-Spindola, J. F.; Miller, N. E. Radical SAM, a Novel Protein Superfamily Linking Unresolved Steps in Familiar Biosynthetic Pathways with Radical Mechanisms: Functional Characterization Using New Analysis and Information Visualization Methods. *Nucleic Acids Res.* **2001**, *29*, 1097−1106.

(20) Frey, P. A.; Hegeman, A. D.; Ruzicka, F. J. The Radical SAM Superfamily. *Crit. Rev. Biochem. Mol. Biol.* **2008**, *43*, 63−88.

(21) Broderick, J. B.; Duffus, B. R.; Duschene, K. S.; Shepard, E. M. Radical S-Adenosylmethionine Enzymes. *Chem. Rev.* **2014**, *114*, 4229−4317.

(22) Latham, J. A.; Barr, I.; Klinman, J. P. At the Confluence of Ribosomally Synthesized Peptide Modification and Radical S-Adenosylmethionine (SAM) Enzymology. *J. Biol. Chem.* **2017**, *292*, 16397−16405.

(23) Schramma, K. R.; Seyedsayamdost, M. R. Lysine-Tryptophan-Crosslinked Peptides Produced by Radical SAM Enzymes in Pathogenic Streptococci. *ACS Chem. Biol.* **2017**, *12*, 922−927.

(24) Schramma, K. R.; Forneris, C. C.; Caruso, A.; Seyedsayamdost, M. R. Mechanistic Investigations of Lysine-Tryptophan Cross-Link

Formation Catalyzed by Streptococcal Radical S-Adenosylmethionine Enzymes. *Biochemistry* **2018**, *57*, 461−468.
(25) Mitchell, A. L.; Attwood, T. K.; Babbitt, P. C.; Blum, M.; Bork, P.; Bridge, A.; Brown, S. D.; Chang, H.-Y.; El-Gebali, S.; Fraser, M. I.; Gough, J.; Haft, D. R.; Huang, H.; Letunic, I.; Lopez, R.; Luciani, A.; Madeira, F.; Marchler-Bauer, A.; Mi, H.; Natale, D. A.; Necci, M.; Nuka, G.; Orengo, C.; Pandurangan, A. P.; Paysan-Lafosse, T.; Pesseat, S.; Potter, S. C.; Qureshi, M. A.; Rawlings, N. D.; Redaschi, N.; Richardson, L. J.; Rivoire, C.; Salazar, G. A.; Sangrador-Vegas, A.; Sigrist, C. J. A.; Sillitoe, I.; Sutton, G. G.; Thanki, N.; Thomas, P. D.; Tosatto, S. C. E.; Yong, S.-Y.; Finn, R. D. InterPro in 2019: Improving Coverage, Classification and Access to Protein Sequence Annotations. *Nucleic Acids Res.* **2019**, *47*, D351−D360.
(26) Fleuchot, B.; Gitton, C.; Guillot, A.; Vidic, J.; Nicolas, P.; Besset, C.; Fontaine, L.; Hols, P.; Leblond-Bourget, N.; Monnet, V.; Gardan, R. Rgg Proteins Associated with Internalized Small Hydrophobic Peptides: A New Quorum-Sensing Mechanism in Streptococci. *Mol. Microbiol.* **2011**, *80*, 1102−1119.
(27) Chang, J. C.; LaSarre, B.; Jimenez, J. C.; Aggarwal, C.; Federle, M. J. Two Group A Streptococcal Peptide Pheromones Act through Opposing Rgg Regulators to Control Biofilm Development. *PLoS Pathog.* **2011**, *7*, No. e1002190.
(28) Samen, U. M.; Eikmanns, B. J.; Reinscheid, D. J. The Transcriptional Regulator RovS Controls the Attachment of *Streptococcus agalactiae* to Human Epithelial Cells and the Expression of Virulence Genes. *Infect. Immun.* **2006**, *74*, 5625−5635.
(29) Chang, J. C.; Jimenez, J. C.; Federle, M. J. Induction of a Quorum Sensing Pathway by Environmental Signals Enhances Group A Streptococcal Resistance to Lysozyme. *Mol. Microbiol.* **2015**, *97*, 1097−1113.
(30) Cook, L. C.; Federle, M. J. Peptide Pheromone Signaling in Streptococcus and Enterococcus. *FEMS Microbiol Rev.* **2014**, *38*, 473−492.
(31) Junges, R.; Salvadori, G.; Shekhar, S.; Åmdal, H. A.; Periselneris, J. N.; Chen, T.; Brown, J. S.; Petersen, F. C. A Quorum-Sensing System That Regulates *Streptococcus pneumoniae* Biofilm Formation and Surface Polysaccharide Production. *mSphere* **2017**, *2*, e00324−17.
(32) Perez-Pascual, D.; Monnet, V.; Gardan, R. Bacterial Cell−Cell Communication in the Host via RRNPP Peptide-Binding Regulators. *Front. Microbiol.* **2016**, *7*, 706.
(33) Markowitz, V. M.; Chen, I. M.; Palaniappan, K.; Chu, K.; Szeto, E.; Pillay, M.; Ratner, A.; Huang, J.; Woyke, T.; Huntemann, M.; Anderson, I.; Billis, K.; Varghese, N.; Mavromatis, K.; Pati, A.; Ivanova, N. N.; Kyrpides, N. C. IMG 4 Version of the Integrated Microbial Genomes Comparative Analysis System. *Nucleic Acids Res.* **2014**, *42*, D560−D567.
(34) Gerlt, J. A.; Bouvier, J. T.; Davidson, D. B.; Imker, H. J.; Sadkhin, B.; Slater, D. R.; Whalen, K. L. Enzyme Function Initiative Enzyme Similarity Tool (EFI-EST): A web tool for generating protein sequence similarity networks. *Biochim. Biophys. Acta, Proteins Proteomics* **2015**, *1854*, 1019−1037.
(35) Gerlt, J. A. Genomic Enzymology: Web Tools for Leveraging Protein Family Sequence-Function Space and Genome Context to Discover Novel Functions. *Biochemistry* **2017**, *56*, 4293−4308.
(36) Caruso, A.; Bushin, L. B.; Clark, K. A.; Martinie, R. J.; Seyedsayamdost, M. R. Radical Approach to Enzymatic β-Thioether Bond Formation. *J. Am. Chem. Soc.* **2019**, *141*, 990−997.
(37) Clark, K. A.; Bushin, L. B.; Seyedsayamdost, M. R. Aliphatic Ether Bond Formation Expands the Scope of Radical SAM Enzymes in Natural Product Biosynthesis. *J. Am. Chem. Soc.* **2019**, *141*, 10610−10615.
(38) Caruso, A.; Martinie, R. J.; Bushin, L. B.; Seyedsayamdost, M. R. Macrocyclization via an Arginine-Tyrosine Crosslink Broadens the Reaction Scope of Radical S-Adenosylmethionine Enzymes. *J. Am. Chem. Soc.* **2019**, *141*, 16610−16614.
(39) Bolotin, A.; Quinquis, B.; Renault, P.; Sorokin, A.; Ehrlich, S. D.; Kulakauskas, S.; Lapidus, A.; Goltsman, E.; Mazur, M.; Pusch, G. D.; Fonstein, M.; Overbeek, R.; Kyprides, N.; Purnelle, B.; Prozzi, D.; Ngui, K.; Masuy, D.; Hancy, F.; Burteau, S.; Boutry, M.; Delcour, J.; Goffeau, A.; Hols, P. Complete Sequence and Comparative Genome Analysis of the Dairy Bacterium *Streptococcus thermophilus*. *Nat. Biotechnol.* **2004**, *22*, 1554−1558.
(40) Bintsis, T. Lactic Acid Bacteria as Starter Cultures: An Update in Their Metabolism and Genetics. *AIMS Microbiol.* **2018**, *4*, 665−684.
(41) Hols, T.; Hancy, F.; Fontaine, L.; Grossiord, B.; Prozzi, D.; Leblond-Bourget, N.; Decaris, B.; Bolotin, A.; Delorme, C.; Dusko Ehrlich, S.; Guédon, E.; Monnet, V.; Renault, P.; Kleerebezem, M. New Insights in the Molecular Biology and Physiology of *Streptococcus thermophilus* Revealed by Comparative Genomics. *FEMS Microbiol. Rev.* **2005**, *29*, 435−463.
(42) Mitchell, T. J. The Pathogenesis of Streptococcal Infections: From Tooth Decay to Meningitis. *Nat. Rev. Microbiol.* **2003**, *1*, 219−230.
(43) Abranches, J.; Zeng, L.; Kajfasz, J.; Palmer, S.; Chakraborty, B.; Wen, Z.; Richards, V.; Brady, L.; Lemos, J. Biology of Oral Streptococci. *Microbiol. Spectrum*. 2018, *6*. DOI: 10.1128/microbiolspec.GPP3-0042-2018.
(44) Delorme, C.; Bartholini, C.; Luraschi, M.; Pons, N.; Loux, V.; Almeida, M.; Guédon, E.; Gibrat, J.-F.; Renault, P. Complete Genome Sequence of the Pigmented *Streptococcus thermophilus* Strain JIM 8232. *J. Bacteriol.* **2011**, *193*, 5581−5582.
(45) Bushin, L. B.; Seyedsayamdost, M. R. Guidelines for Determining the Structures of Radical SAM Enzyme-Catalyzed Modifications in the Biosynthesis of RiPP Natural Products. *Methods Enzymol.* **2018**, *606*, 439−460.
(46) Haft, D. H.; Basu, M. K. Biological Systems Discovery in Silico: Radical S-Adenosylmethionine Protein Families and Their Target Peptides for Posttranslational Modification. *J. Bacteriol.* **2011**, *193*, 2745−2755.
(47) Goldman, P. J.; Grove, T. L.; Sites, L. A.; McLaughlin, M. I.; Booker, S. J.; Drennan, C. L. X-Ray Structure of an AdoMet Radical Activase Reveals an Anaerobic Solution for Formylglycine Posttranslational Modification. *Proc. Natl. Acad. Sci. U. S. A.* **2013**, *110*, 8519−8524.
(48) Grell, T. A. J.; Goldman, P. J.; Drennan, C. L. SPASM and Twitch Domains in S-Adenosylmethionine (SAM) Radical Enzymes. *J. Biol. Chem.* **2015**, *290*, 3964−3971.
(49) Davis, K. M.; Schramma, K. R.; Hansen, W. A.; Bacik, J. P.; Khare, S. D.; Seyedsayamdost, M. R.; Ando, N. Structures of the peptide-modifying radical SAM enzyme SuiB elucidate the basis for substrate recognition. *Proc. Natl. Acad. Sci. U. S. A.* **2017**, *114*, 10420−10425.
(50) Rea, M. C.; Sit, C. S.; Clayton, E.; O'Connor, P. M.; Whittal, R. M.; Zheng, J.; Vederas, J. C.; Ross, R. P.; Hill, C. Thuricin CD, a Posttranslationally Modified Bacteriocin with a Narrow Spectrum of Activity against *Clostridium difficile*. *Proc. Natl. Acad. Sci. U. S. A.* **2010**, *107*, 9352−9357.
(51) Lohans, C. T.; Vederas, J. C. Structural Characterization of Thioether-Bridged Bacteriocins. *J. Antibiot.* **2014**, *67*, 23−30.
(52) Himes, P. M.; Allen, S. E.; Hwang, S.; Bowers, A. A. Production of Sactipeptides in *Escherichia coli*: Probing the Substrate Promiscuity of Subtilosin A Biosynthesis. *ACS Chem. Biol.* **2016**, *11*, 1737−1744.
(53) Flühe, L.; Knappe, T. A.; Gattner, M. J.; Schäfer, A.; Burghaus, O.; Linne, U.; Marahiel, M. A. The Radical SAM Enzyme AlbA Catalyzes Thioether Bond Formation in Subtilosin A. *Nat. Chem. Biol.* **2012**, *8*, 350−357.
(54) Flühe, L.; Burghaus, O.; Wieckowski, B. M.; Giessen, T. W.; Linne, U.; Marahiel, M. A. Two [4Fe-4S] Clusters Containing Radical SAM Enzyme SkfB Catalyze Thioether Bond Formation during the Maturation of the Sporulation Killing Factor. *J. Am. Chem. Soc.* **2013**, *135*, 959−962.
(55) Bruender, N. A.; Bandarian, V. SkfB Abstracts a Hydrogen Atom from Cα on SkfA to Initiate Thioether Cross-Link Formation. *Biochemistry* **2016**, *55*, 4131−4134.
(56) Bruender, N. A.; Wilcoxen, J.; Britt, R. D.; Bandarian, V. Biochemical and Spectroscopic Characterization of a Radical S-

Adenosyl-L-Methionine Enzyme Involved in the Formation of a Peptide Thioether Cross-Link. *Biochemistry* **2016**, *55*, 2122−2134.
(57) Shi, Y.; Yang, X.; Garg, N.; van der Donk, W. A. Production of Lantipeptides in *Escherichia coli*. *J. Am. Chem. Soc.* **2011**, *133*, 2338−2341.
(58) Dewhirst, F. E.; Chen, T.; Izard, J.; Paster, B. J.; Tanner, A. C. R.; Yu, W.-H.; Lakshmanan, A.; Wade, W. G. The Human Oral Microbiome. *J. Bacteriol.* **2010**, *192*, 5002−5017.
(59) Fontaine, L.; Boutry, C.; de Frahan, M. H.; Delplace, B.; Fremaux, C.; Horvath, P.; Boyaval, P.; Hols, P. A Novel Pheromone Quorum-Sensing System Controls the Development of Natural Competence in *Streptococcus thermophilus* and *Streptococcus salivarius*. *J. Bacteriol.* **2010**, *192*, 1444−1454.
(60) Gardan, R.; Besset, C.; Guillot, A.; Gitton, C.; Monnet, V. The Oligopeptide Transport System is Essential for the Development of Natural Competence in *Streptococcus thermophilus* Strain LMD-9. *J. Bacteriol.* **2009**, *191*, 4647−4655.
(61) Boutry, C.; Wahl, A.; Delplace, B.; Clippe, A.; Fontaine, L.; Hols, P. Adaptor Protein MecA is a Negative Regulator of the Expression of Late Competence Genes in *Streptococcus thermophilus*. *J. Bacteriol.* **2012**, *194*, 1777−1788.
(62) Gardan, R.; Besset, C.; Gitton, C.; Guillot, A.; Fontaine, L.; Hols, P.; Monnet, V. Extracellular Life Cycle of ComS, the Competence-stimulating Peptide from *Streptococcus thermophilus*. *J. Bacteriol.* **2013**, *195*, 1845−1855.
(63) Steinmoen, H.; Teigen, A.; Håvarstein, L. S. Competence-induced Cells of *Streptococcus pneumoniae* Lyse Competence-deficient Cells of the Same Strain During Cocultivation. *J. Bacteriol.* **2003**, *185*, 7176−7183.
(64) Guiral, S.; Mitchell, T. J.; Martin, B.; Claverys, J.-P. Competence-programmed Predation of Noncompetent Cells in the Human Pathogen *Streptococcus pneumoniae*: Genetic Requirements. *Proc. Natl. Acad. Sci. U. S. A.* **2005**, *102*, 8710−8715.
(65) Claverys, J.-P.; Håvarstein, L. S. Cannibalism and Fratricide: Mechanisms and Raisons D'être. *Nat. Rev. Microbiol.* **2007**, *5*, 219−229.
(66) Shankar, E.; Federle, M. J. Quorum Sensing Regulation of Competence and Bacteriocins in *Streptococcus pneumoniae* and *mutans*. *Genes* **2017**, *8*, 15.
(67) Claverys, J.-P.; Martin, B.; Håvarstein, L. S. Competence-induced Fratricide in Streptococci. *Mol. Microbiol.* **2007**, *64*, 1423−1433.
(68) Berg, K. H.; Biørnstad, T. H.; Johnsborg, O.; Håvarstein, L. S. Properties and Biological Role of Streptococcal Fratricins. *Appl. Environ. Microbiol.* **2012**, *78*, 3515−3522.
(69) Havarstein, L. S.; Martin, B.; Johnsborg, O.; Granadel, C.; Claverys, J.-P. New Insights into the Pneumococcal Fratricide: Relationship to Clumping and Identification of a Novel Immunity Factor. *Mol. Microbiol.* **2006**, *59*, 1297−1307.
(70) Babasaki, K.; Takao, T.; Shimonishi, Y.; Kurahashi, K. Subtilosin A, a New Antibiotic Peptide Produced by *Bacillus subtilis* 168: Isolation, Structural Analysis, and Biogenesis. *J. Biochem.* **1985**, *98*, 585−603.
(71) Kawulka, K.; Sprules, T.; McKay, R. T.; Mercier, P.; Diaper, C. M.; Zuber, P.; Vederas, J. C. Structure of subtilosin A, an antimicrobial peptide from *Bacillus subtilis* with unusual posttranslational modifications linking cysteine sulfurs to alpha-carbons of phenylalanine and threonine. *J. Am. Chem. Soc.* **2003**, *125*, 4726−4727.
(72) Kawulka, K. E.; Sprules, T.; Diaper, C. M.; Whittal, R. M.; McKay, R. T.; Mercier, P.; Zuber, P.; Vederas, J. C. Structure of Subtilosin A, a Cyclic Antimicrobial Peptide from Bacillus Subtilis with Unusual Sulfur to α-Carbon Cross-Links: Formation and Reduction of α-Thio-α-Amino Acid Derivatives. *Biochemistry* **2004**, *43*, 3385−3395.
(73) Sit, C. S.; McKay, R. T.; Hill, C.; Ross, R. P.; Vederas, J. C. The 3D Structure of Thuricin CD, a Two-Component Bacteriocin with Cysteine Sulfur to α-Carbon Cross-Links. *J. Am. Chem. Soc.* **2011**, *133*, 7680−7683.
(74) Sit, C. S.; van Belkum, M. J.; McKay, R. T.; Worobo, R. W.; Vederas, J. C. The 3D Solution Structure of Thurincin H, a Bacteriocin with Four Sulfur to α-Carbon Crosslinks. *Angew. Chem., Int. Ed.* **2011**, *50*, 8718−8721.
(75) Mo, T.; Ji, X.; Yuan, W.; Mandalapu, D.; Wang, F.; Zhong, Y.; Li, F.; Chen, Q.; Ding, W.; Deng, Z.; Yu, S.; Zhang, Q. Thuricin Z: A Narrow-Spectrum Sactibiotic that Targets the Cell Membrane. *Angew. Chem., Int. Ed.* **2019**, *58*, 18792−18797.
(76) Balty, C.; Guillot, A.; Fradale, L.; Brewee, C.; Boulay, M.; Kubiak, X.; Benjdia, A.; Berteau, O. Ruminococcin C, an Anti-Clostridial Sactipeptide Produced by a Prominent Member of the Human Microbiota *Ruminococcus gnavus*. *J. Biol. Chem.* **2019**, *294*, 14512−14525.
(77) Chiumento, S.; Roblin, C.; Kieffer-Jaquinod, S.; Tachon, S.; Leprétre, C.; Basset, C.; Aditiyarini, D.; Olleik, H.; Nicoletti, C.; Bornet, O.; Iranzo, O.; Maresca, M.; Hardré, R.; Fons, M.; Giardina, T.; Devillard, E.; Guerlesquin, F.; Couté, Y.; Atta, M.; Perrier, J.; Lafond, M.; Duarte, V. Ruminococcin C, a Promising Antibiotic Produced by a Human Gut Symbiont. *Sci. Adv.* **2019**, *5*, eaaw9969.

https://dx.doi.org/10.1021/jacs.0c05546
J. Am. Chem. Soc. 2020, 142, 16265−16275